Published in Physical Review Letters 48, issue 9, 6732-6735, 1993
which should be used for any reference to this work

Local epitaxy of Ag on $Bi_2Sr_2CaCu_2O_{8+x}$(001)

P. Schwaller, P. Aebi, J. Osterwalder, and L. Schlapbach
Institut de Physique, Université de Fribourg, CH-1700 Fribourg, Switzerland

M. Shimoda, T. Mochiku, and K. Kadowaki
National Research Institute for Metals, 2-3-12, Nakameguro, Meguro-Ku, Tokyo 153, Japan

Thin films of Ag have been deposited onto cleaved $Bi_2Sr_2CaCu_2O_{8+x}$(001) surfaces at room temperature. Ag 3*d* x-ray photoelectron diffraction experiments show very poor local order at coverages of up to 7 Å. For higher Ag coverages, a distinct diffraction pattern is forming, indicative of local epitaxy in the form of two domains of Ag(110) patches with one diagonal of the rectangular surface unit cell aligned along the substrate *a* axis. Comparison with previously published scanning-tunneling-microscopy results [Y. S. Luo *et al.*, Phys. Rev. B **46**, 1114 (1992)] leads us to the conclusion that Ag epitaxy is promoted by local disruption of the substrate upon initial Ag deposition.

Of all interfaces between metals and copper-oxide-based high-temperature superconductors (HTC's), the one between silver and $Bi_2Sr_2CaCu_2O_{8+x}$ has become particularly important because of its occurrence in several early technological applications of HTC materials.[1] Although silver is believed to be little reactive on such interfaces, there are indications that high coverages on single-crystal samples lead to partial reduction of Cu underneath the surface, probably induced by oxygen depletion of near-surface Cu-O planes.[2]

Recently, a microscopic mechanism for adatom-induced disruption of $Bi_2Sr_2CaCu_2O_{8+x}$(001) surfaces has been proposed on the basis of scanning-tunneling-microscopy (STM) and x-ray photoelectron spectroscopy (XPS) results.[3] In brief, it is suggested that the Bi-O surface terminating layer is metastable, and that the liberated cohesion energy of forming Ag islands suffices to locally induce an oxidation to Bi_2O_3, which requires a transport of oxygen from deeper layers (especially the Cu-O layers) to the surface. The metastable character of the top Bi-O layer is supported by the observation that Ne sputtering, Ag deposition, and heat treatment all lead to similar modifications in surface chemistry and electronic structure.[4]

The STM images taken by Luo, Yang, and Weaver[3] on cleaved $Bi_2Sr_2CaCu_2O_{8+x}$(001) surfaces show atomic resolution, and the incommensurate modulation of the bulk structure[5,6] is clearly seen to persist at the surface, leading to stripes along the *a* axis, spaced at roughly 25 Å.[7–10] At submonolayer Ag coverage the formation of circular islands of typically 25 Å in diameter is observed which appear to be aligned along the stripes. Atomic resolution is not obtained, and it is thus not clear where the islands are anchored with respect to the modulation. At higher coverages the islands start to coalesce, and at 20 Å coverage the mean island size approaches 100 Å. The STM data give no information on crystallinity, composition, or orientation of these islands.

In order to have a microscopic view of the internal structure of these interfaces we have measured the Ag 3*d* x-ray photoelectron diffraction (XPD).[11] Our group has recently demonstrated that collecting the diffraction patterns over almost the full 2π solid angle above the surface considerably enhances the power of this technique for structural determination, and in particular that it enables us to study rather complex systems with or without long-range order and with several inequivalent atom positions.[12,13] The strong forward focusing of the photoelectrons by near-neighbor atomic potentials[11] produces distinct maxima on a two-dimensional angular distribution map measured above the surface. Each emission site thus projects the crystal structure onto the measurement hemisphere,[14,15] and projections from inequivalent sites are simply superimposed.

We have prepared clean $Bi_2Sr_2CaCu_2O_{8+x}$(001) surfaces by scotch tape cleaving in ultrahigh vacuum at pressures in the low 10^{-10} mbar range, which were then characterized by low-energy electron diffraction (LEED) and XPS. The crystal growth is described elsewhere.[16] Ag was deposited at 300 K by evaporation from a hot filament. The deposition rate was monitored by means of a quartz microbalance, and we give the coverages in terms of the monitor readings. Since we want to compare our results to those obtained with the STM by Luo, Yang, and Weaver,[3] we had to verify that they use the same coverage scale as we do. Measuring Ag-to-substrate ratios by means of quantitative XPS and considering variations in Cu 2*p* spectra assured us that our coverage scale deviates from that of Refs. 2 and 3 by less than 25%.

In order to measure the photoelectron diffraction patterns, the sample is transferred to a computer controlled two-axis goniometer. In 3600 angular steps the photoelectron emission direction is swept over much of the solid angle above the crystal,[14] up to polar angles of 78°. At each setting a spectrum of Ag 3*d* and of Bi 4*f*, excited by Mg $K\alpha$ radiation, is measured and the intensities are extracted by curve fitting. The whole procedure is fully

automated and takes, for these two signals, about 50 h. No sample degradation is observed during this time.

Figures 1(a)–1(c) show the Bi $4f$ emission patterns for Ag coverages of 7, 21, and 42 Å, given in stereographic projection and with a linear gray scale ranging from minimum (black) to maximum (white) intensity within each pattern. All patterns shown are raw data with no symmetry averaging performed. The center of the intensity map represents normal emission whereas the outer circle draws the azimuth of a polar angle of 90° in the stereographic projection. The intensity distributions of the Bi $4f$ patterns are characteristic for the emission from a covered substrate: low intensities for grazing exit angles due to an increased path length through the adsorbate. Furthermore we do not notice a significant change of the Bi $4f$ intensity distribution with coverage. Forward-focusing peak positions compare well with those of the clean substrate published earlier by our group.[17] It means that the average Bi emitter within the escape depth does not have an ordered Ag environment. This is consistent with the formation of Ag clusters as observed by Luo, Yang, and Weaver. Ag cluster formation is also indicated by LEED, where we found no difference between the clean and the Ag covered crystal, except for a progressing attenuation of the substrate spots.

Figures 1(d)–1(f) present the corresponding Ag $3d$ diffraction patterns for Ag coverages of 7, 21, and 42 Å.

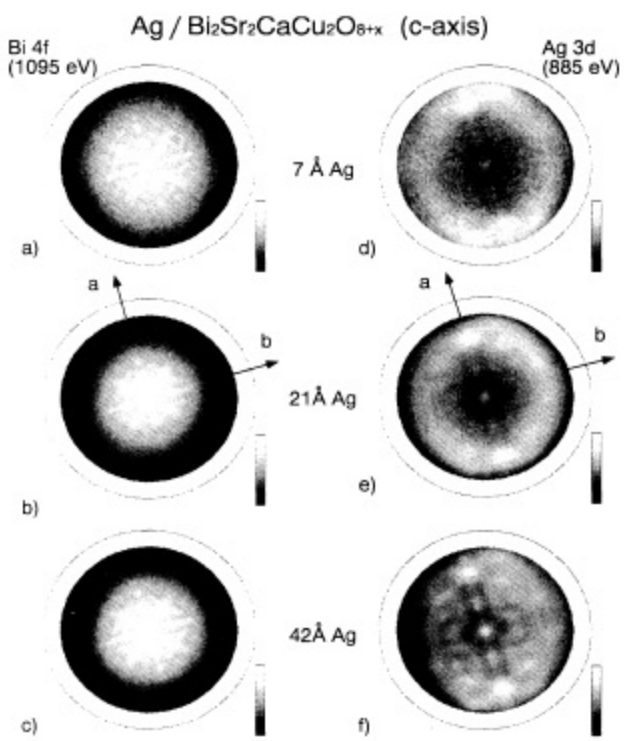

FIG. 1. Bi $4f$ (a)–(c) and Ag $3d$ (d)–(f) photoelectron diffractograms for Ag coverages of 7, 21, and 42 Å, measured at electron kinetic energies of 1095 eV for Bi and 885 eV for Ag. The vectors **a** and **b** represent the crystallographic directions of the substrate.

We find very poor local order for coverages up to 7 Å, i.e., far beyond the regime where the STM sees island alignment. However, for coverages of 20 Å and more a distinct pattern is forming, dominated by three forward-focusing spots at polar angles of 62° and 0° aligned along the a axis. At 42 Å the pattern is clearly twofold symmetric and exhibits a considerable amount of fine structure. Inspired by the polar positions of the forward-focusing maxima, and by a comparison with the XPD pattern obtained from a clean Pt(110) surface,[14] we considered a structural model consisting of two domains of (110)-oriented clusters, rotated by 109°, both of which have one diagonal of the rectangular surface unit cell aligned with the a axis of the substrate [Fig. 2(a)]. Given these clusters we performed single-scattering cluster (SSC) calculations using spherical-wave corrections and proper p and f photoemission final states.[18,19] Figure 3 shows the experimental pattern obtained at 84 Å Ag coverage, which is very similar to that at 42 Å, together with the domain-averaged result of a SSC calculation with a total number of 222 atoms distributed over four layers in each domain. The agreement is strikingly good, if one remembers that single-scattering models largely overestimate forward-focusing anisotropies and peak widths.[20] All the fine structure of the experimental pattern is accurately reproduced, which is clear evidence that Ag forms local (110) patches. The two main maxima at 62° off normal are thus identified as forward focusing by [011] nearest neighbors within the Ag clusters.

This finding is very remarkable for several reasons. First of all it is puzzling that Ag first grows in islands (STM) without or with poor local order (XPD), and then at higher coverage, when many islands have coalesced (STM) local order starts to form. Second, the very open (110) orientation is found. In contrast, on Cu(001) the more densely-packed (111)-oriented growth is observed.[21]

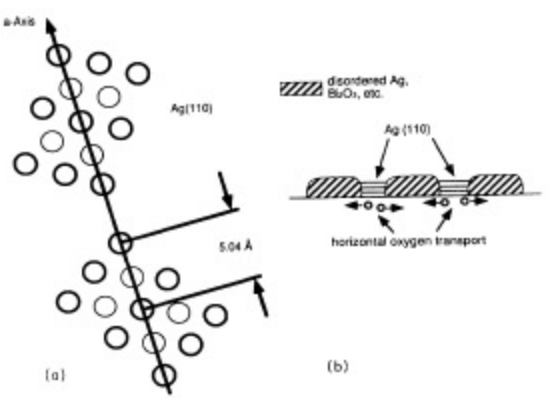

FIG. 2. (a) Structural model consisting two domains of (110)-oriented clusters, rotated by 109°, both of which have one diagonal of the rectangular surface unit cell aligned with the a axis of the substrate. The mismatch between the lattice constant (5.40 Å) of the unmodulated Bi-Sr-Ca-Cu-O (2:2:1:2) and the diagonal of the Ag(110) unit cell (5.01 Å) is 7%. (b) Suggested model of the ordered Ag(110) patches forming directly on the substrate between islands of disordered material (Ag, Bi_2O_3, etc.).

On GaAs(110) Ag forms crystallites of (110) orientation [22] with facets corresponding to (111)-type surfaces. In this case, the lattice match does not appear to play an important role in determining the overlayer growth since the orientation does not follow simple geometric considerations.[22] It seems more important for the Ag overlayer to match the symmetry of the substrate than to optimize the lattice match. This is evident also in the present case from the fact that the azimuthal orientation of these patches is sensitive to the modulated structure of the substrate, as we have a clear alignment with the crystal *a* axis and not with the *b* axis.

With these observations in mind one can now try to understand the morphology of the film during growth. In the submonolayer range small islands are aligned along the *z* axis (STM), i.e., initial condensation of Ag clusters occurs predominantly on one particular phase of the modulation. These clusters are not oriented, and we do not know their internal structure and composition. According to the model by Luo, Yang, and Weaver[3] they are surrounded by oxygen-enriched Bi_2O_3-type precipitates. The ordered Ag(110) patches definitely cannot form on top of these disordered clusters. It is furthermore unlikely that originally disordered Ag at the interface, which is being covered by further Ag and maybe by Bi_2O_3, becomes ordered, and we are thus led to the conclusion that the (110) patches form directly on the substrate at places between the islands [Fig. 2(b)].

XPD can provide here quantitative information on what proportion of the Ag is present in locally epitaxial patches: Figure 4(a) shows azimuthal Ag 3*d* intensity curves at a polar angle of 62°, i.e., cutting through the intense forward-focusing maxima, for four different Ag coverages. The absolute anisotropy of these maxima, defined as $(I_{max}-I_{min})/I_{max}$, is 22% at 84 Å coverage. Figure 4(b) shows the anisotropies as a function of coverage. We notice that for anisotropies of the order of 20% XPD shows clearly the two Ag(110) domains whereas for anisotropies below 10% the two (110) domains are not very distinct. The anisotropy of the corresponding [011] nearest-neighbor maxima from a well-ordered single-crystal Ag(110) sample has not been measured, but we know from the comparison with other noble-metal and transition-metal samples[11,14,23] that this number lies between 50 and 60%. From this and in consideration of the two Ag(110) domains we can conclude that our 22% anisotropy corresponds to 50–60% of the total amount of Ag, the rest being disordered and contributing a uniform background to the XPD patterns.

A substantial part of the substrate is thus capable to promote local epitaxial growth of Ag, but only after a

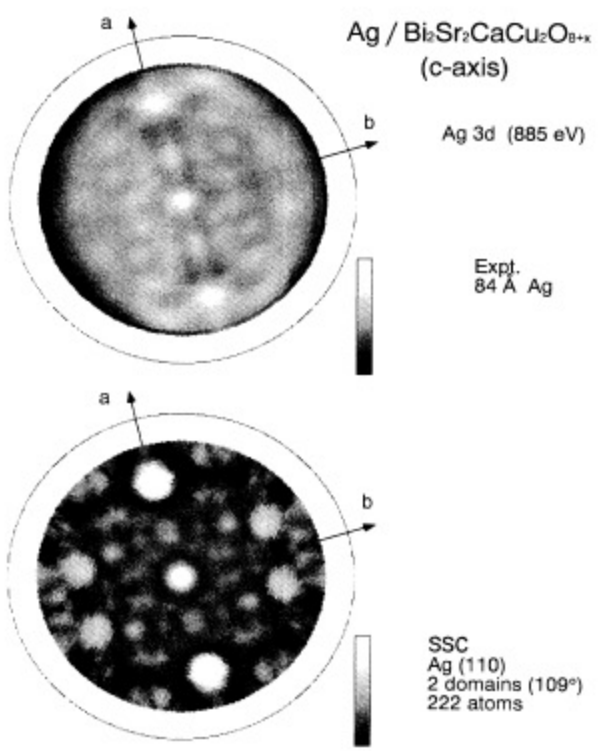

FIG. 3. Experimental Ag 3*d* pattern obtained at 84 Å Ag coverage (top), together with the domain-averaged result of a SSC calculation with a total number of 222 atoms distributed over four layers in each domain (bottom). The intensity maxima of the calculated pattern are cut to enhance contrast. (See text).

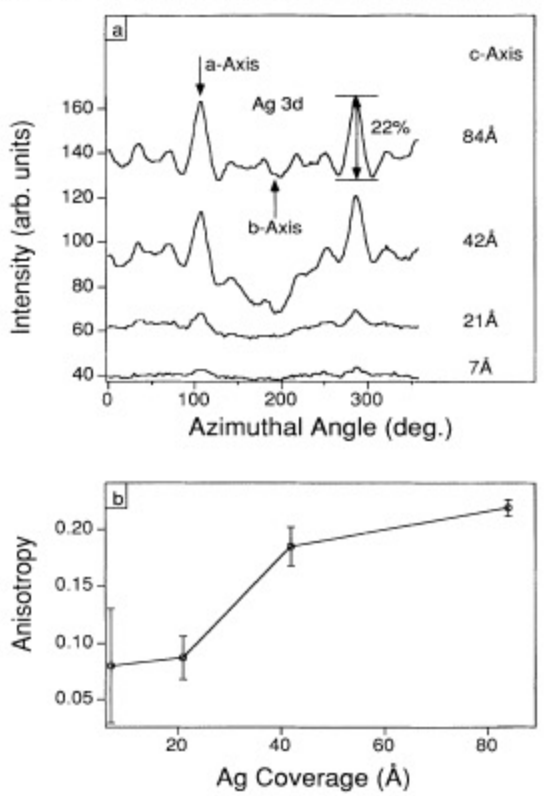

FIG. 4. (a) Azimuthal Ag 3*d* intensity curves at a polar angle of 62° for Ag coverages on $Bi_2Sr_2CaCu_2O_{8+x}$ of 7, 21, 42, and 84 Å. The absolute anisotropy of these maxima, defined as $(I_{max}-I_{min})/I_{max}$, is 22% at 84 Å coverage. (b) Absolute anisotropies of the maxima at the polar angle of 62° as a function of Ag coverage.

pretreatment which seems to be associated with the formation of the initial disordered clusters. Considering the lattice mismatch one may speculate as to the character of this pretreatment. The diagonal of the Ag(110) surface unit cell is 5.01 Å, while the lattice constant of the substrate is 5.40 Å along the a axis for unmodulated $Bi_2Sr_2CaCu_2O_{8+x}$(001). The average misfit is a fairly high 7%, and only at few places of the modulation it comes to within acceptable 1–2 %. The modulation is strongly related to the local oxygen content.[5,6] According to the model by Luo, Yang, and Weaver[3] the initial Ag islands leach oxygen from deeper layers by promoting Bi_2O_3 precipitation. Our results suggest that there is not only vertical, but also horizontal transport of oxygen, which leads to oxygen-deficient surface regions that serve as templates for the local growth of Ag(110).

Finally, we would like to point out that the combination of STM and XPD is particularly powerful in solving such complex interface problems.

This work was supported by the Swiss National Foundation project NFP 30. We thank D. Naumović, R. Fasel, and H. A. Aebischer for useful discussions and for their support during the experiments.

[1]D. R. Dietderich, B. Ullmann, H. C. Freyhardt, J. Kase, H. Kumakura, K. Togano, and H. Maeda, Jpn. J. Appl. Phys. **29**, L1100 (1990).

[2]H. M. Meyer III, D. M. Hill, T. J. Wagener, J. H. Weaver, C. F. Gallo, and K. C. Goretta, J. Appl. Phys. **65**, 3130 (1989).

[3]Y. S. Luo, Y.-N. Yang, and J. H. Weaver, Phys. Rev. B **46**, 1114 (1992).

[4]P. A. P. Lindberg, Z.-X. Shen, I. Lindau, W. E. Spicer, C. B. Eom, and T. H. Geballe, Appl. Phys. Lett. **53**, 529 (1988).

[5]Y. Le Page, W. R. McKinnon, J.-M. Tarascon, and P. Barboux, Phys. Rev. B **40**, 6810 (1989).

[6]A. Yamamoto, M. Onoda, E. Takayama-Muromachi, F. Izumi, T. Ishigaki, and H. Asano, Phys. Rev. B **42**, 4228 (1990).

[7]We found some inconsistency in the labeling of the axes with respect to the observed stripe pattern. We adopt the definition given by Ref. 6 for the bulk structure, which has the modulation along the b axis. The stripes are then parallel to the a axis.

[8]M. D. Kirk, J. Nogami, A. A. Baski, D. B. Mitzi, A. Kapitulnik, T. H. Geballe, and C. F. Quate, Science **242**, 1673 (1988).

[9]P. A. P. Lindberg, Z.-X. Shen, B. O. Wells, D. B. Mitzi, I. Lindau, W. E. Spicer, and A. Kapitulnik, Appl. Phys. Lett. **53**, 2563 (1988).

[10]C. K. Shih, R. M. Feenstra, J. R. Kirtley, and G. V. Chandrashekhar, Phys. Rev. B **40**, 2682 (1989).

[11]For a review see, e.g., C. S. Fadley, in *Synchrotron Radiation Research: Advances in Surface Science,* edited by R. Z. Bachrach (Plenum, New York, 1989); W. F. Egelhoff, Jr., Crit. Rev. Solid State Mater. Sci. **16**, 213 (1990); S. A. Chambers, Surf. Sci. Rep. **16**, 261 (1992).

[12]D. Naumović, A. Stuck, T. Greber, J. Osterwalder, and L. Schlapbach, Surf. Sci. **269/270**, 719 (1992); **277**, 235 (1992); D. Naumović, J. Osterwalder, A. Stuck, P. Aebi, and L. Schlapbach, *ibid.* **287/288**, 950 (1993).

[13]A. Fischer, R. Fasel, J. Osterwalder, A. Krozer, and L. Schlapbach, Phys. Rev. Lett. **70**, 1493 (1993).

[14]J. Osterwalder, T. Greber, A. Stuck, and L. Schlapbach, Phys. Rev. B **44**, 13 764 (1991).

[15]T. Greber, J. Osterwalder, D. Naumović, A. Stuck, S. Hüfner, and L. Schlapbach, Phys. Rev. Lett. **69**, 1947 (1992).

[16]T. Mochiku and K. Kadowaki, in *Electronic Properties and Mechanisms of High T_c Superconductors,* edited by T. Oguchi, K. Kadowaki, and T. Sasaki (Elsevier Science, New York, 1992).

[17]M. Shimoda, T. Greber, J. Osterwalder, and L. Schlapbach, Physica C **196**, 236 (1992).

[18]J. J. Rehr and R. C. Albers, Phys. Rev. B **41**, 8139 (1990).

[19]D. J. Friedman and C. S. Fadley, J. Electron Spectrosc. Relat. Phenom. **51**, 689 (1990).

[20]S. Y. Tong, H. C. Poon, and D. R. Snider, Phys. Rev. B **32**, 2096 (1985); M.-L. Xu, J. J. Barton, and M. A. Van Hove, *ibid.* **39**, 8275 (1989); H. A. Aebischer, T. Greber, J. Osterwalder, A. P. Kaduwela, D. J. Friedman, G. S. Herman, and C. S. Fadley, Surf. Sci. **239**, 261 (1990).

[21]D. Naumović, doctoral thesis, Université de Fribourg, 1993.

[22]B. M. Trafas, Y.-N. Yang, R. L. Siefert, and J. H. Weaver, Phys. Rev. B **43**, 14 107 (1991); Y.-N. Yang, Y. S. Luo, and J. H. Weaver, *ibid.* **45**, 3606 (1992).

[23]D. Naumović, A. Stuck, T. Greber, J. Osterwalder, and L. Schlapbach, Phys. Rev. B **47**, 7462 (1993).

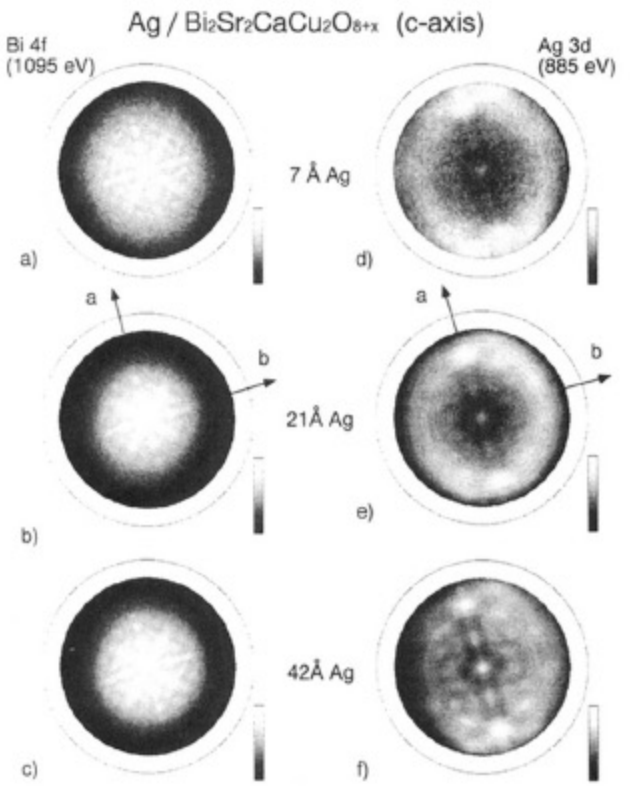

FIG. 1. Bi 4*f* (a)–(c) and Ag 3*d* (d)–(f) photoelectron diffractograms for Ag coverages of 7, 21, and 42 Å, measured at electron kinetic energies of 1095 eV for Bi and 885 eV for Ag. The vectors **a** and **b** represent the crystallographic directions of the substrate.

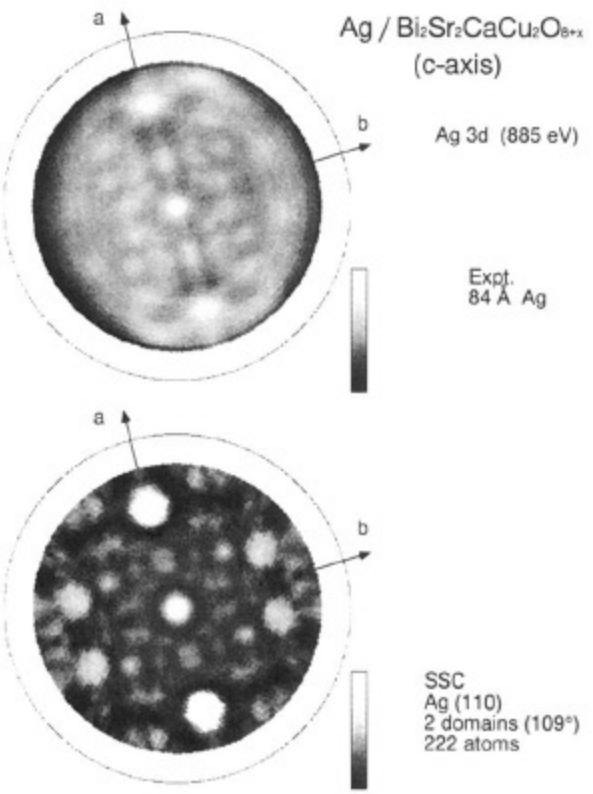

FIG. 3. Experimental Ag 3*d* pattern obtained at 84 Å Ag coverage (top), together with the domain-averaged result of a SSC calculation with a total number of 222 atoms distributed over four layers in each domain (bottom). The intensity maxima of the calculated pattern are cut to enhance contrast. (See text).